Can Low-Energy Electrons Affect High-Energy Physics Accelerators?

R. Cimino,[1,2] I. R. Collins,[2] M. A. Furman,[3] M. Pivi,[4] F. Ruggiero,[2] G. Rumolo,[5] and F. Zimmermann[2]

[1]*LNF-INFN, Frascati, Italy*
[2]*CERN, Geneva, Switzerland*
[3]*LBNL, Berkeley, California 94720, USA*
[4]*SLAC, Stanford, California 94025, USA*
[5]*GSI, Darmstadt, Germany*

(Received 10 February 2004; published 29 June 2004)

Present and future accelerators' performances may be limited by the electron cloud (EC) effect. The EC formation and evolution are determined by the wall-surface properties of the accelerator vacuum chamber. We present measurements of the total secondary electron yield (SEY) and the related energy distribution curves of the secondary electrons as a function of incident-electron energy. Particular attention has been paid to the emission process due to very low-energy primary electrons (<20 eV). It is shown that the SEY approaches unity and the reflected electron component is predominant in the limit of zero primary incident electron energy. Motivated by these measurements, we have used state-of-the-art EC simulation codes to predict how these results may impact the production of the electron cloud in the Large Hadron Collider, under construction at CERN, and the related surface heat load.

DOI: 10.1103/PhysRevLett.93.014801 PACS numbers: 29.27.Bd, 41.75.Lx, 79.20.Hx

In 1989 an instability driven by photoelectrons was observed at the National Laboratory for High Energy Physics (KEK) Photon Factory. It was not until 1994 that its origin was correctly identified as due to the formation of an electron cloud (EC) [1,2]. Since then several proton-storage rings [3,4], electron-positron colliders [4], and synchrotron radiation (SR) sources, when operating with positrons, have reported similar beam instabilities which are now understood to be due to a coupling between the beam and an EC. Deleterious effects of the EC include interference with diagnostic devices, coupled-bunch coherent beam instabilities, and single-bunch incoherent effects such as emittance increase. In general, the EC is significant in machines with intense, closely spaced, short, positively charged bunches, and vacuum chambers of relatively small transverse dimensions. In the cases of the *B* factories PEP-II and KEKB, the EC in the positron rings led to important operational limitations and to an intense search for mitigating mechanisms [4–6]. An EC related effect is the beam-induced electron multipacting, and it can be explained as follows: a few "seed" electrons may be generated by ionization of the residual gas or by photoemission. These electrons are accelerated by the bunch electric field in the direction perpendicular to the beam motion. If the bunch charge and the bunch spacing satisfy a certain condition, the traversal time of the electron across the vacuum chamber equals the time interval between successive bunches, and a resonance condition is established. If, in addition, the effective secondary electron yield (SEY) at the chamber is larger than unity, the electron population grows rapidly in time with successive bunch passages, leading to a high electron cloud density. A closely related phenomenon, called trailing-edge multipacting, has also been observed for a single proton bunch at the Los Alamos Proton-Storage Ring (PSR) when the beam intensity exceeds a certain threshold [7]. It could prove important for the future Spallation Neutron Sources (SNS). In the case of positron storage rings, and for the CERN Large Hadron Collider (LHC) [8,9], the EC is mainly seeded by photoelectrons emitted off the chamber walls by the SR [10] produced by the beam as it traverses the bending magnets in the ring. For the other hadron machines, the seed mechanism is typically ionization of residual gas and/or electron generation by stray beam particles striking the chamber walls at grazing angles. In almost all cases, however, the secondary emission process is the crucial ingredient in amplifying the energy and the intensity of the electrons of the EC.

A novel EC effect is expected at the LHC, namely, an excess power deposition on the vacuum chamber beam screen due to the EC bombardment. Since the LHC magnets are superconducting, being operated at 1.9 K, it is important to understand and control the heat load on the cryogenic system. To protect the cold bore (vacuum envelope) from SR irradiation and image currents, a beam screen (BS) is inserted. The BS is held at a temperature between 5 and 20 K. The available BS cooling capacity is exceeded if the EC-induced heat load surpasses 1 to 1.5 W/m [11] in any of the two rings, and in this case, the EC will limit the achievable machine performance. During the past several years the EC has been studied experimentally at several machines including the two *B* factories, BEPC, PSR, PS, SPS, and BNL Relativistic Heavy Ion Collider by means of dedicated instruments and computer simulations such as POSINST, ECE and ECLOUD (see Ref. [4] for details). These simulations, which take as input the secondary emission yield as a

 0031-9007/04/93(1)/014801(4)$22.50

function of the energy E_0 of the incident electron, $\delta(E_0)$, and the energy distribution of the emitted secondaries, $d\delta/dE(E_0)$, among other ingredients, have had some notable successes in modeling many aspects of the EC, including single- and multibunch instabilities for positron rings with short bunches, and trailing-edge multipacting in the PSR so that a reasonable degree of confidence now exists in the predictions of these codes and in the understanding of the EC that has thereby been obtained. However, the simulations have until now been limited also by uncertainties in the measurements of the SEY at low incident-electron energy ($E_0 \lesssim 20$ eV). In this Letter it is shown that, in order to correctly predict any EC-induced additional heat load in the LHC, it is essential to determine accurately the energy distribution of the emitted secondary electrons, $d\delta/dE$, and the relative composition of the emitted secondary electrons, i.e., the relative ratio of backscattered to true secondaries. The SEY for actual LHC beam screen samples, measured down to unprecedentedly low energies and here presented, shows that, as the incident-electron energy E_0 is lowered below $\sim$10 eV, the SEY does not decrease monotonically, as previously fitted [4], but rather shows an upturn, leading to a high value of the SEY at zero energy, namely, $\delta(0) \sim 1$. The importance of studying the properties of low-energy primary electrons interacting with the industrially prepared sample is underscored by the notion that, according to simulations, when an EC develops, the energy distribution of the electrons impinging on the wall peaks at very low energy ($\lesssim$20 eV) [12]. The data here presented are fed into the aforementioned computer simulations codes.

The simulations confirm the importance of the very low-energy electrons for correctly estimating EC effects and for addressing the operational reliability of future machines like the LHC, the GSI-SIS (Gesellschaft für Schwer-Ionenforschung-Schwer Ionen), the SNS, or linear-collider damping rings. The EDC at low primary energy was analyzed by a dedicated experimental apparatus, presently at CERN, which is described in detail elsewhere [13]. In brief, a combination of a cryopump and an ultrahigh vacuum μ-metal chamber reduces residual magnetic field near the sample and allows operation in a vacuum better than 10^{-10} Torr without bakeout. The energy distribution curves (EDCs) were collected by a Spectaleed Omicron retarding field Analyzer, specially modified to be able to collect angle-integrated EDCs at very low impinging electron energy. The e^- beam was always smaller than 1 mm^2 in transverse cross-sectional area and stable (both in current and position) for energies between 30 and 350 eV, as confirmed by a line profile and by stability tests done using a homemade 1 mm slot Faraday cup. The sample could be kept at a constant temperature between 8 and 400 K. A bias voltage was applied, in order to measure secondary emission for very low primary electron energies, while keeping the gun in a region where it was stable and focused. The samples studied were all part of the real chamber surface in the LHC. We find it reasonable to assume that the surfaces of other technical materials used for vacuum chambers exhibit the same general behavior as the data presented here. Testing this assumption calls for more systematic and broader investigations of the type described in this Letter. Figure 1 shows a subset of EDCs taken as a function of primary energy from an as-received Cu sample at 10 K after it was conditioned by bombarding with more than 1 C/cm^2 of 400 eV e^- in an open geometry. This e^- dosing is known to produce surface modifications leading to a stable surface [4] (i.e., a surface with a SEY that no longer changes with further electron dosing). From the spectra in Fig. 1, it is clear that at primary energies higher than 100 eV the main contribution to the EDC is given by the secondary electrons emitted with 0 to 15 eV kinetic energy and only a small fraction is due to electrons elastically reflected from the surface. As the primary energy gets lower, the ratio between reflected and secondary electrons increases, until reflection becomes dominant for primary energies below 20 eV. From the available data it is possible, by simple numerical integration, to extract the ratio between *true secondary* and *elastically reflected* electrons for each primary energy. We do not separately consider *rediffused* electrons, since at low primary energy the separation between true secondaries and rediffused electrons becomes rather arbitrary. Rather, we consider all the electrons emitted between 0 eV up to the onset of the clear elastic peak at the primary electron energy as true-secondary electrons, while the integral under this peak gives the amount of elastically reflected electrons. In Fig. 2 we present SEY measurements of the same sample as used for measuring the EDC, taken before, during, and after scrubbing. First, the curves show that the behavior at low primary energies is largely independent of δ_{max} and of the degree of scrubbing. From the EDC data of Fig. 1 and the fully scrubbed SEY curve of Fig. 2 we can determine the yield of reflected electrons per incident primary electron. This is shown as a fit and decomposition in Fig. 2, for the case

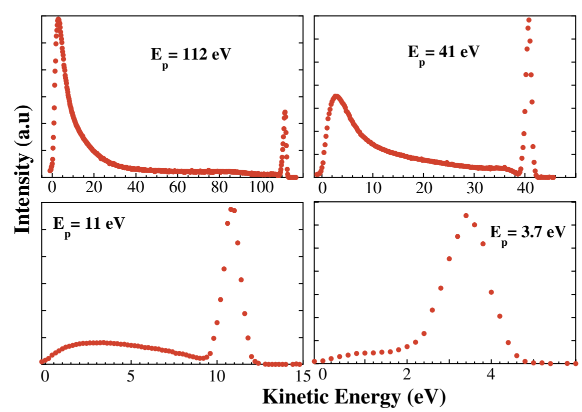

FIG. 1 (color online). Measured EDCs of a fully scrubbed Cu surface at about 10 K for different primary electron energies at normal incidence.

of the fully scrubbed surface. At low energy most of the impinging electrons are reflected by the Cu surface, resulting in a SEY value that approaches unity in the limit of vanishing primary energy. The value of the observed SEY minimum and the corresponding energy depend on the actual sample and on its conditions (temperature, scrubbing, etc.), while the overall shape of the SEY curve is preserved and a SEY value close to unity has been measured at low E_0 in all cases. The data demonstrate the importance of the reflected electrons at low primary energy and suggest, for the first time in this context, that low-energy electrons may have long survival time inside the accelerator vacuum chambers due to their high reflectivity. This notion may explain why in the KEK *B* factory [4] and in the CERN SPS [14] a memory effect has been observed, namely, the EC buildup observed during the passage of a bunch train is enhanced by the passage of a preceding bunch train, even if the time interval between the two trains is quite long (500 ns in the SPS and 1 μs at KEKB). The EC simulation codes have been described in detail elsewhere [4]. To simulate LHC, the two main sources of electrons are given by photoemission from SR and by secondary emission from electrons hitting the walls.

The SEY for perpendicular incidence at a primary energy E_0 is described as the sum of two components, $\mathrm{SEY} = \delta_{\mathrm{el}} + \delta_{\mathrm{true}}$, each of which is approximated by fits to measurements [4]. The true-secondary component is $\delta_{\mathrm{true}}(x) = \delta^*_{\max} s x/(s - 1 + x^s)$, where $x = E/E^*_{\max}$ and where the value $s \approx 1.35$ has been obtained from several measured data sets [15]. There are only two free parameters, namely, the energy at which the true yield is maximum, $E^*_{\max}$, and the effective maximum secondary emission yield $\delta^*_{\max}$. The measurements of elastic reflection reported in this Letter are very well parametrized by $\delta_{\mathrm{el}}(E) = (\sqrt{E} - \sqrt{E + \epsilon_0})^2/(\sqrt{E} + \sqrt{E + \epsilon_0})^2$, with only one fit parameter ϵ_0. The above formula for δ_{el} can be obtained from a simple quantum-mechanical model [16], considering a plane-wave electron wave function incident on a negative potential step of depth ϵ_0 (here 150 eV). The

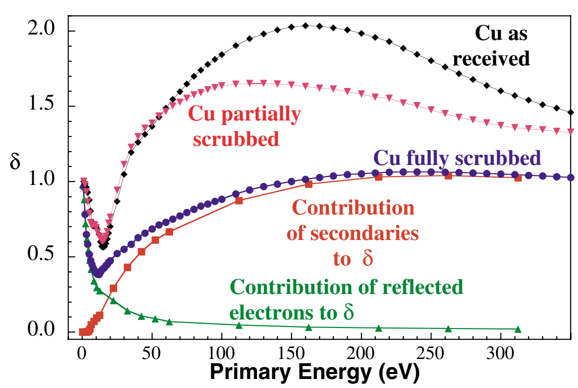

FIG. 2 (color online). Total SEY (δ) at normal incidence and the contribution of secondary and reflected electrons from a fully scrubbed Cu surface at about 10 K as a function of E_0.

expression for δ_{el} introduces a minimum in the total SEY curve, as seen in Fig. 2. It always yields a reflectivity of 1 in the limit that E approaches 0 eV, consistent with the measurements presented above.

We remark that previously used parametrizations either ignored the elastic component or used a phenomenological formula for δ_{el} [4,5,15] obtained by simple extrapolation down to $E_0 = 0$, of available data which were taken with higher incident-electron energy E_0 than those discussed here. Although the results of such simulations [17] did show a substantial increase of the EC power deposition relative to those in which δ_{el} was wholly neglected, the amount of such an increase was generally different than what is presented in this Letter, and the details of the mechanism were not well understood.

SEY parametrizations, with and without elastic reflection, are shown for an energy range between 0 and 300 eV in the inset of Fig. 3. The model with elastic reflection is the best fit to the data (Fig. 2) of the fully scrubbed surface with ($\delta^*_{\max} = 1.06$ and $E_{\max} = 262$ eV). We have used such a fit to extrapolate, according to the above equations, SEY curves with different values of $\delta^*_{\max}$ and $E_{\max}$ eV, using them as input to simulations, modeling the behavior of an LHC beam, consisting of 72 bunches with 25 ns spacing through an arc dipole chamber. Heat loads, simulated as a function of bunch intensity, are shown in Fig. 3 for a true-secondary maximum yield of $\delta^*_{\max} = 1.7$. Such value of $\delta^*_{\max}$ is expected during the intermediate stages of the scrubbing process. It is clear that it is important to correctly model the SEY at low energy. In fact, without considering reflected low-energy electrons (full line), the simulated heat load is well within the available cooling budget in all calculated cases, but this is no longer true if we include in the calculation the high reflectivity of low-energy electrons, as reported in this Letter. This specific result suggests the need of particular care in the LHC commissioning scenario. To

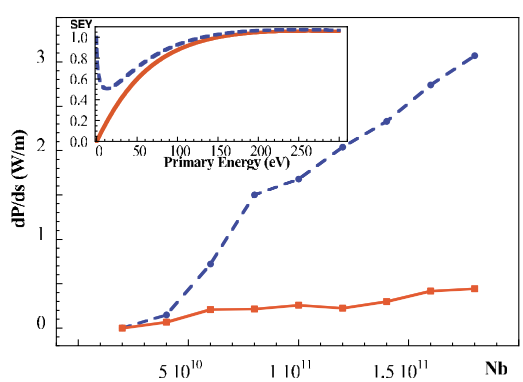

FIG. 3 (color online). Simulated average heat load in an LHC dipole magnet as a function of proton bunch population at 0.45 TeV, calculated by extrapolating the best fit to the data of Fig. 2 (shown in the inset) for a SEY with $\delta^*_{\max} = 1.7$ and $E_{\max} = 240$ eV, considering the elastic reflection (dashed line) or ignoring it (full line).

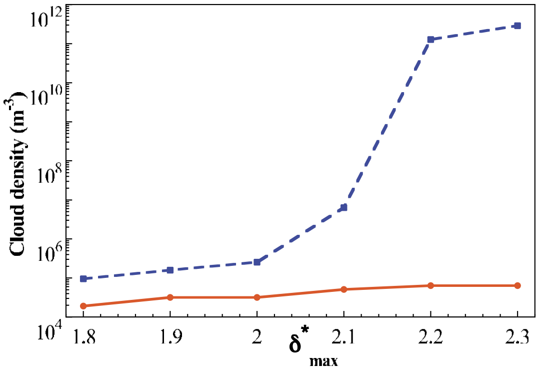

FIG. 4 (color online). Simulated average EC density in a field-free section of the GSI-SIS18 as a function of δ_{max}, comparing the cases with (dashed line) and without (full line) elastic reflection.

present a second example, we now discuss the case of the synchrotron SIS18 at GSI, which will be upgraded so as to become an injector for the planned synchrotron SIS100. One of the possible operation scenarios presently foreseen requires the acceleration in the SIS18 of 4×10^{10} U^{73+} (packed in four 80 ns long bunches with a 100 ns spacing) to 1 GeV/u. Figure 4 shows that the modeling of elastic reflection based on our data lowers the δ^*_{max} threshold for the onset of the electron cloud to $\sim$2.2, whereas no significant EC is to be expected for δ^*_{max} values beyond 2.3 without elastic reflection. The implications of the new parametrization here proposed for low-energy electron SEY is currently under study for other present and planned accelerators.

In conclusion, the experimental data and the simulations clearly demonstrate the importance of elastic electron reflection at low energies, whose probability is shown, in this study, to approach unity in the limit of zero incident energy. The data indicate that low-energy electrons are long-lived in the accelerator vacuum chamber, explaining the puzzling observations of memory effects seen at the KEK B factory and at the CERN SPS. Calculations including the measured elastic reflection predict a significantly higher heat load for the LHC arcs than previously expected and a possible EC formation in the heavy ion synchrotron SIS18 at GSI when upgraded to deliver the required currents for the future facilities. The results presented here, therefore, call for a general reexamination of EC predictions for all present and future accelerators, including linear-collider damping rings.

The authors are indebted to V. Baglin, G. Bellodi, M. Blaskiewicz, M. Dapor, D. Schulte, and P. Strubin. This work was partially supported by INFN-group V and by the U.S. DOE under Contracts No. DE-AC03-76SF00515 and No. DE-AC03-76SF00098.

[1] M. Izawa, Y. Sato, and T. Toyomasu, Phys. Rev. Lett. **74**, 5044 (1995).
[2] K. Ohmi, Phys. Rev. Lett. **75**, 1526 (1995).
[3] M. Blaskiewicz, M. A. Furman, M. Pivi, and R. J. Macek, Phys. Rev. ST Accel. Beams **6**, 014203, 2003, and references therein.
[4] Proceedings ECLOUD'02, CERN Yellow Report No. CERN-2002-001, 2002, and references therein.
[5] *Proceedings of the International Workshop on Multibunch Instabilities in Future Electron and Positron Accelerators (MBI'97)*, edited by Y. H. Chin (KEK, Tsukuba, 1997), Proc. 97-17.
[6] *Proceedings of the International Workshop on Two-Stream Instabilities in Particle Accelerators and Storage Rings, Tsukuba, Japan, 2001* (KEK, Tsukuba, 2001) (http:// conference.kek.jp/two-stream/).
[7] R. Macek *et al.*, in *Proceedings of the 2001 Particle Accelerator Conference "PAC2001," Chicago, 2001*, edited by P. Lucas and S. Webber (IEEE, Piscataway, NJ, 2001), p. 688 (http:// pac2001.aps.anl.gov/).
[8] LHC Study Group, Author *et al.*, "*The Large Hadron Collider—Conceptual Design*," CERN Report No. CERN/AC/95-05, 1995.
[9] F. Zimmermann, CERN LHC Project/Report No. 95, 1997.
[10] R. Cimino, I. R. Collins, and V. Baglin, Phys. Rev. ST Accel. Beams **2**, 063201 (1999).
[11] U. Wagner, Proceedings of Chamonix XIII (to be published).
[12] F. Zimmermann, in Proceedings of Chamonix XI (CERN Report No. CERN-SL-2001-003 DI, 2001).
[13] R. Cimino and I. R. Collins, Appl. Surf. Sci. (to be published).
[14] J. M. Jimenez *et al.*, CERN Report No. LHC P.R. 632, 2003.
[15] M. A. Furman and M. T. F. Pivi, Phys. Rev. ST Accel. Beams **5**, 124404 (2003).
[16] M. Blaskiewicz (private communication).
[17] M. A. Furman, LBNL Report No. LBNL-41482/CBP Note 247/LHC P. R. 180, 1998.